

# Analysis of Nozzle Lip and Backflow Expansion of a Small Hydrazine Thruster

Iain D. Boyd\* and J. P. W. Stark†

*University of Southampton, Southampton, England, United Kingdom*

Results are presented for computations made with the direct simulation Monte Carlo method for the expansion of the thick boundary layer of a small nozzle. The objective in the investigation is to assess the boundary-layer characteristics that most affect the flow properties of the expanding gas. In the computations, large degrees of species separation and thermal nonequilibrium are observed as the gas expands around the nozzle lip. These aspects of the flow indicate the necessity of treating the problem through a discrete particle approach. Assessment is made of the sensitivity of the calculated results to the form of the boundary layer initially assumed. It is found that the amount of backflow is related to the flow temperature close to the wall. Therefore, the opportunity presents itself for the reduction of the impingement potential of such thrusters through appropriate design considerations. Experimental procedures for verification of the type of computations undertaken in the current study are discussed. It is proposed that the calculations made in the backflow region offer the best opportunity for direct comparison.

## Introduction

AN increasing amount of interest is being shown in the accurate determination of the backflow regions exhausting from small satellite thrusters. This interest has arisen partly as a result of the growing requirements for improved budgeting of on-board satellite resources and partly as a consequence of the deleterious effects of thruster plume impingement encountered on several missions. In recent years, both experimental<sup>1,2</sup> and theoretical<sup>2,3</sup> investigations have been undertaken. In the prediction of possible impingement occurring between the plume backflow and the surfaces of the spacecraft, the flow near the nozzle lip has been shown to be of great importance. For the small nozzle studies in Refs. 1 and 3, it is reported that the flow properties in this region do not correspond to those predicted using conventional Navier-Stokes boundary-layer techniques. It is therefore necessary to calculate such flows in greater detail.

The authors previously have reported on calculations made in the isentropic core of a small hydrazine thruster.<sup>4</sup> Both continuum and discrete particle solutions were generated. It was found that errors arose as a consequence of applying the continuum solution techniques to the noncontinuum transition flow regime of the plume. The differences provided by the various methods considered were quite large. Hence, the aerodynamic characteristics of drag force and heat transfer were underpredicted in the continuum results by up to a factor of 2. In the boundary-layer expansion and backflow regions of the plume flowfield, larger and more significant departures between discrete particle and continuum calculations are to be expected due to extreme rarefaction effects. In the present study, report is made of calculations undertaken in the laminar boundary layer and in the region around the nozzle lip of the same hydrazine thruster considered in Ref. 4. Similar flowfields have been examined previously for a large solid rocket motor<sup>5</sup> and for the flow of argon out of a small tube.<sup>6</sup> The thruster considered has very small dimensions, with an

exit radius of a few millimeters. Consequently, the Reynolds number of the flow is low (about  $3.6 \times 10^3$ ) so that the boundary-layer thickness occupies up to 35% of the exit plane. For further details on this thruster see Ref. 4.

Computations are made solely with a discrete particle technique. The one employed here is the direct simulation Monte Carlo method (DSMC), which has been developed by Bird.<sup>7</sup> In this method, the large number of molecules in a real gas is simulated by a much smaller statistical population of model particles. Intermolecular collisions are treated on a probabilistic basis and are decoupled from molecular motion over a time step which is small compared to the mean time between collisions. The region of physical space to be modeled is spanned by a network of cells that are used to simulate local flow conditions and are used as a location for the output of data. The dimensions of each cell should be less than the local mean free path. Macroscopic flow properties are obtained by averaging the molecular quantities over sample sizes, which are sufficiently large to reduce statistical fluctuations to an acceptable level. For a recent review of the method and its application, see Ref. 8.

The presence of molecules in the backflow region of the plume arises mainly from thermal scattering. The DSMC method is, therefore, an appropriate solution technique as the flow is modeled at the molecular level. It is anticipated that little useful information would be obtained from continuum formulations that assumed perfect thermal equilibrium and neglect scattering effects. In the following, the application of the DSMC method to the boundary-layer expansion of the hydrazine thruster is considered.

## Computations

The thruster chamber conditions and information on the gas mixture in the boundary layer are listed in Table 1. In the following calculations, both the vibrational and chemical states of the gas are assumed to be frozen. The transfer of energy between the translational and rotational modes is simulated through use of the Larsen-Borgnakke model<sup>9</sup> with a constant collision number of 5 for each species. The simulation scheme employed is the Time Counter method of Bird.<sup>7</sup> At the time of this study, this method offered the best numerical performance<sup>10</sup> and incurred the lowest statistical fluctuations<sup>11</sup> when compared with alternative simulation schemes.

The computations of the boundary layer are begun inside the nozzle lip. In Figs. 1, the computational domain and regional subdivision are shown. Because of the dramatic

Received March 3, 1989; revision received Feb. 5, 1990. Copyright © 1990 by the American Institute of Aeronautics and Astronautics, Inc. All rights reserved.

\*Graduate Student, Department of Aeronautics and Astronautics; currently at NASA Ames Research Center, Moffett Field, CA. Member AIAA.

†Senior Lecturer, Department of Aeronautics and Astronautics. Member AIAA.

**Table 1 Thruster chamber conditions and information on the gas mixture in the boundary layer**

Thruster		Boundary layer	
Area ratio	63	Fraction of H <sub>2</sub>	0.4933
Nozzle half-angle	15 deg	Fraction of N <sub>2</sub>	0.2987
Stagnation pressure	$1.57 \times 10^6$ Pa	Fraction of NH <sub>3</sub>	0.2080
Stagnation temperature	1170 K	Molecular weight	12.9
Exit Mach number	5.78	Ratio of specific heats	1.37

rarefaction experienced by the gas as it expands around the lip (it is expected that the density will decrease by several orders of magnitude), the domain is divided into a number of distinct regions. In each of these regions, different physical scaling factors and decoupling time steps are employed. The flux of molecules across cell boundaries is always exactly matched. The final grid structure together with the time steps and scaling factors have been obtained through a number of preliminary numerical experiments. Although these procedures have previously been applied successfully to similar flowfields,<sup>5</sup> they are quite inefficient. The number of simulated molecules entering the backflow region is small. Therefore, in order to accumulate sample sizes that are sufficiently large to attain statistical fluctuations at an acceptable level, a substantial number of time steps for the entire flowfield must be marched through. This, unfortunately, means that a significant amount of computational effort is wasted in unnecessary recalculation of the more dense regions of the flow.

One of the primary aims of the present work is to assess the influence of several of the boundary-layer characteristics on the expanded flowfield structure. In Refs. 5 and 6, the initial density, velocity, and temperature profiles inside the nozzle were provided by continuum calculation methods. Although the effect of nozzle geometry is considered in Ref. 6, the sensitivity of the results presented to the input data is not analyzed in any of the previous studies. In the work reported here, the effect of varying the initial distributions for velocity and temperature are investigated. In addition, the dependence on the gas/surface interaction model is considered. It is the purpose of the study to gain further understanding of the physical processes that occur in such flows. In particular, it is the intention to indicate the aspects of the boundary layer that are of greatest importance in defining the flow quantities of interest in impingement analysis.

For the present application, the uncertainties associated with the specification of the boundary layer are large. This is attributable primarily to the rarefied nature of the thruster, the solution of which would ideally involve a DSMC calculation of the entire nozzle. Such an undertaking would require vast amounts of computational resources and lies beyond the scope of this work. In view of these difficulties, it was decided to employ simplistic solutions for the laminar boundary layer. Therefore, a flat-plate velocity profile, a uniform temperature

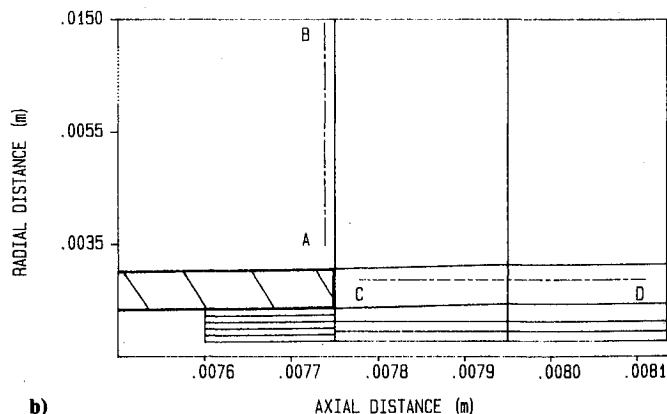
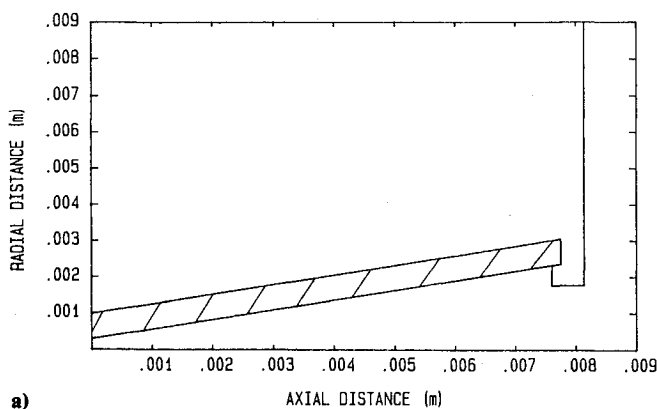
**Table 2 Initial conditions input into DSMC calculations**

Case	Density	Velocity	Temperature	Surface
1	Laminar	Flat plate	Uniform (197 K)	Diffuse (197 K)
2	Laminar	Flat plate	Uniform (197 K)	Diffuse (855 K)
3	Laminar	Flat plate	Laminar	Diffuse (855 K)
4	Laminar	Flat plate	Laminar	Diffuse (300 K)
5	Laminar	Flat plate	Laminar	Specular
6	Laminar	Power law	Laminar	Diffuse (855 K)

profile, and a typical laminar boundary-layer profile for density were initially assumed for input into the DSMC calculations. The nozzle wall was modeled as a diffusely reflecting surface with complete energy accommodation corresponding to the adiabatic temperature. In making these assumptions, it is to be remembered that the primary interest is the investigation of the response of the computed results to variations in the initial conditions. Therefore, a number of solutions for the flowfield were generated in which these input data were varied. Details of the conditions considered are listed in Table 2. For these cases, the effect of the input temperature profile, the surface temperature at the nozzle wall, the gas/surface interaction model, and the initial velocity profile are all systematically investigated. The nonuniform profiles assumed for velocity, density, and temperature are shown in Figs. 2-4. The data are plotted such that a boundary-layer position of 1 corresponds to the nozzle wall and the position 0 lies at the inviscid edge of the flow. The sensitivity of the solutions has been characterized by examination of the flow properties in the nozzle exit plane and along the lines AB and CD of Figs. 1. In the exit plane, basic flow properties such as the velocity profile and the degree of thermal nonequilibrium are of interest. In the outer regions of the flowfield, attention is confined to those quantities that affect impingement analysis such as dynamic pressure, species abundance, and flow angle. In the discussions that follow, it should be noted that the conditions given in case 3 are considered the most realistic.

### Results in the Nozzle Exit Plane

Figure 5 shows the exit plane velocity profiles obtained with the six initial conditions investigated. The profiles for cases 1, 2, and 3 are similar. The result taken from case 4 indicates that some influence is felt for the diffuse wall temperature

**Fig. 1 Computational domain for backflow showing regional subdivision.**

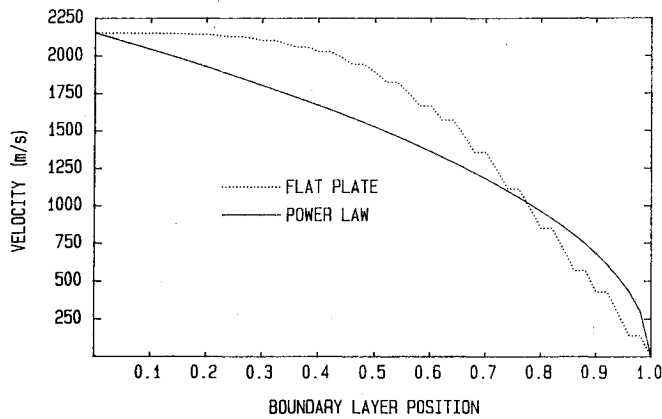


Fig. 2 Velocity profiles assumed in the laminar boundary layer.

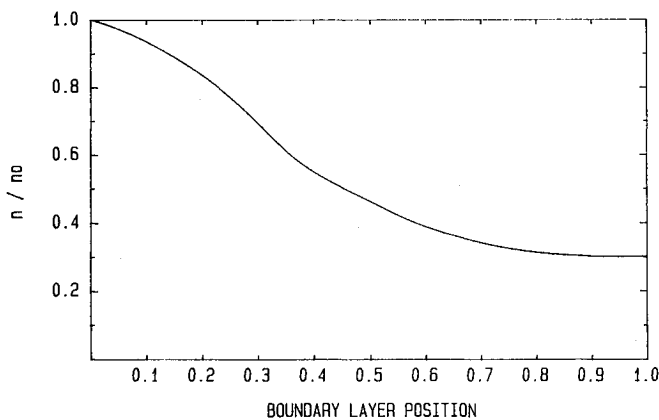


Fig. 3 Density profile assumed in the laminar boundary layer.

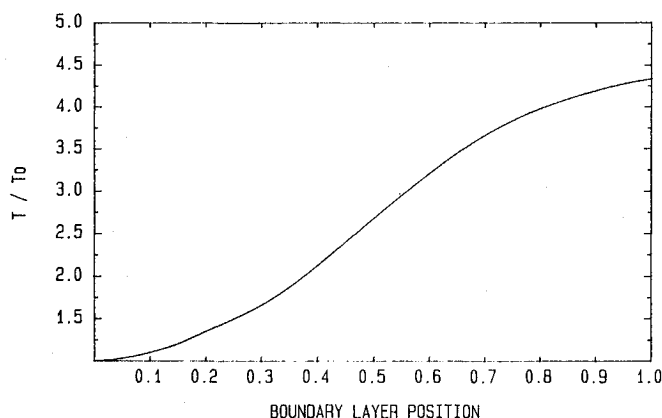


Fig. 4 Temperature profile assumed in the laminar boundary layer.

assumed. The use of specular wall reflection (case 5) leads to higher flow velocities in regions close to the nozzle. Finally, it may be observed that the relationship between the profile obtained for case 6 and that for case 3 is similar to that found between the initial velocity input conditions plotted in Fig. 4. In general, the influence of the assumed wall conditions extends some 60% from the nozzle wall into the laminar boundary layer.

The degree of thermal nonequilibrium in the nozzle exit plane may be assessed by examination of Fig. 6, in which the temperature of the various thermal modes obtained for case 3 are shown. It is found that close to the inviscid edge of the boundary the modes are in thermal equilibrium. However, as the nozzle wall is approached, significant departure between the translational and rotational modes is observed. At the

same time, good agreement is found for the axial and radial translational modes in most of the exit plane.

The relative concentrations by number density for the various species remains invariant throughout the majority of the boundary layer for five of the cases. The exception occurs for case 4, the results for which are shown in Fig. 7. The condition investigated sets the wall temperature below that of the gas (see Table 2). At small distances from the wall, a rather unexpected phenomenon is observed. The concentration of hydrogen, which is the lightest constituent, is seen to fall, whereas those for both ammonia and nitrogen increase. This result is presumed to arise from thermal diffusion effects, which have been discussed by Bird.<sup>12</sup> The trend of this effect is similar to that first noted in the calculations of Moss et al.<sup>13</sup> In

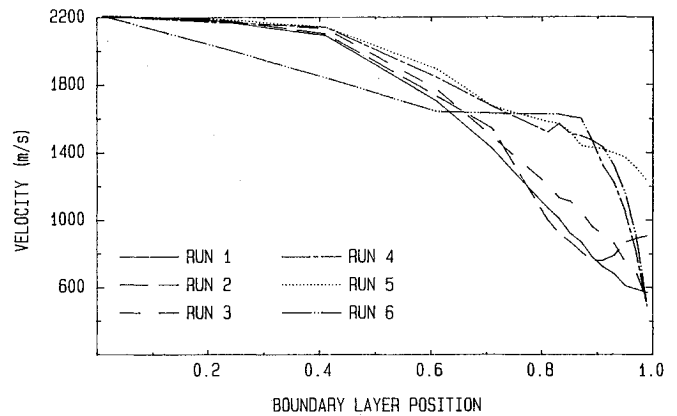


Fig. 5 Velocity profiles in the nozzle exit plane.

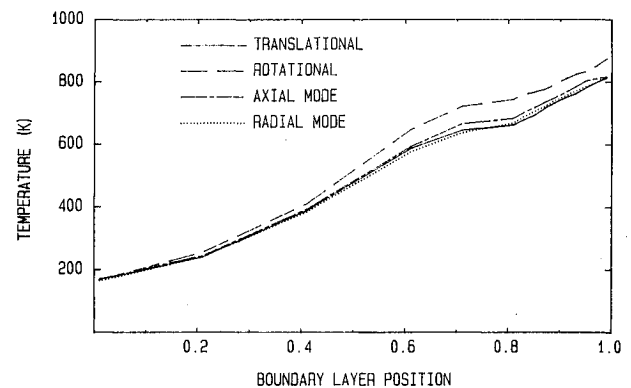


Fig. 6 Thermal nonequilibrium in the nozzle exit plane from case 3.

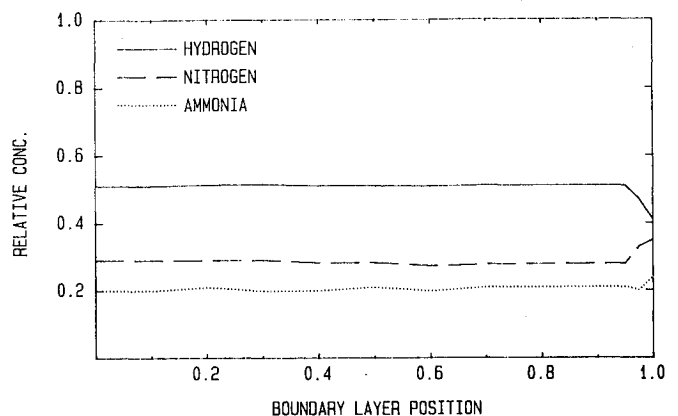


Fig. 7 Relative species concentrations in the nozzle exit plane from case 4.

Ref. 13, it is reported that the concentration of heavier species increased unexpectedly at a small distance from a cold surface suffering impingement from a hot gas.

### Results in the Region Forward of the Nozzle Lip

The flow properties along the line CD in Fig. 1 are now considered. This portion of the flowfield originates in the expansion of the boundary layer. It is therefore expected that the effect of the nozzle wall condition will decrease along CD. In Fig. 8, the dynamic pressure is plotted for each of the simulations undertaken. It is clear that although cases 3-6 give good agreement, the results for cases 1 and 2 are markedly different. Such trends are hardly surprising as the introduction of

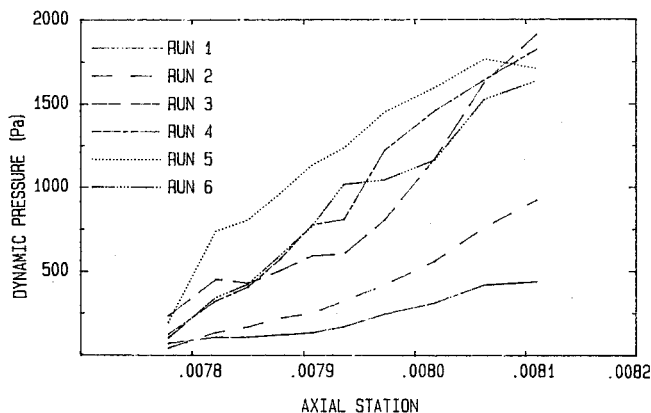


Fig. 8 Dynamic pressure forward of the nozzle lip.

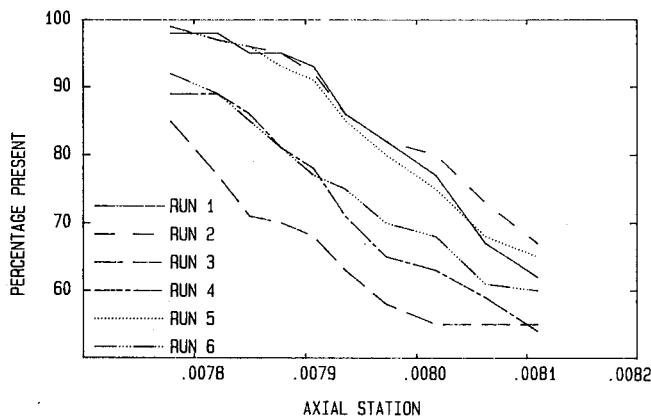


Fig. 9 Hydrogen concentration forward of the nozzle lip.

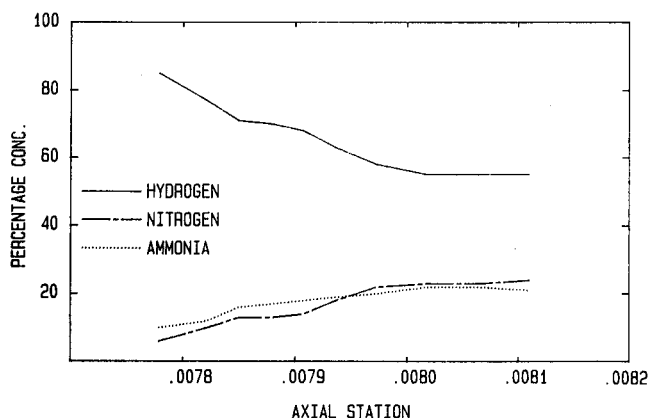


Fig. 10 Relative species abundance forward of the nozzle lip from case 3.

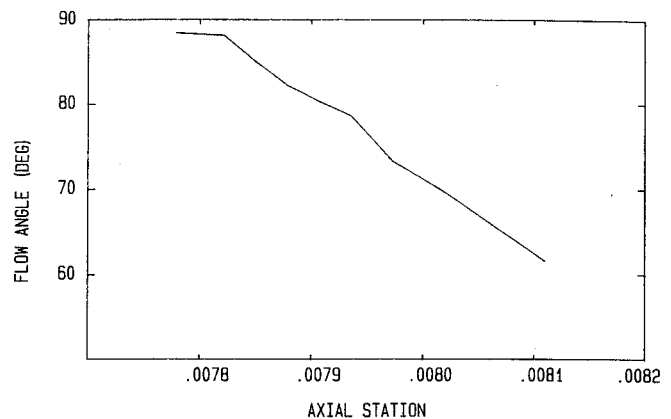


Fig. 11 Flow angle forward of the nozzle lip from case 3.

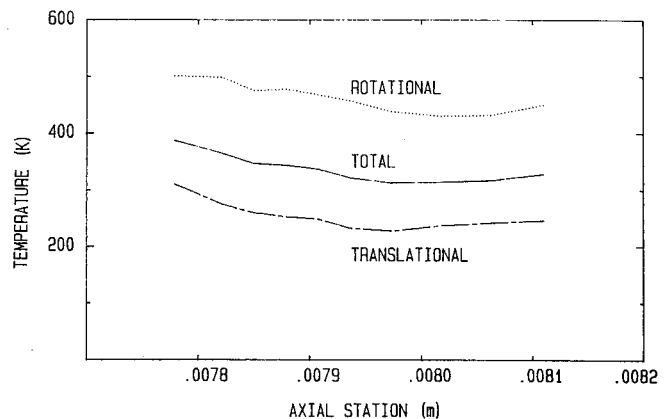


Fig. 12 Thermal nonequilibrium forward of the nozzle lip from case 3.

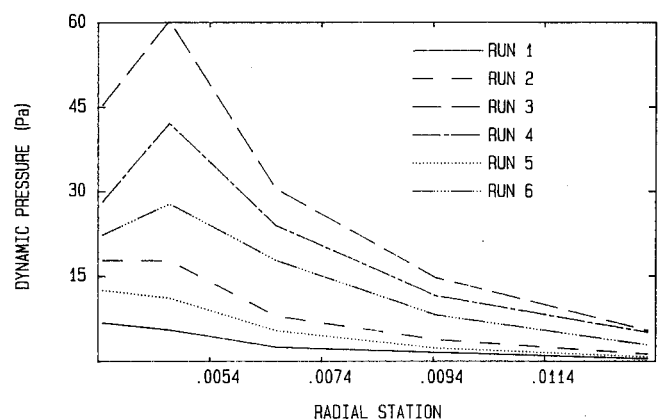


Fig. 13 Dynamic pressure in the backflow region.

a temperature profile at the nozzle wall would certainly be expected to influence the flowfield structure. It may be concluded from these results that larger impingement forces are associated with a boundary layer having a temperature profile giving rise to high values at the nozzle wall.

It is interesting to note that the introduction of specular reflection (case 5) seems to have little impact on the results shown in Fig. 8. However, examination of Fig. 9, in which the relative species concentration of hydrogen is shown, suggests that this is not, in fact, the case. In these results, it is evident that the specular wall results more closely resemble those given under the conditions prevailing in cases 1 and 2. Careful inspection of the calculations revealed that the assumption of specular reflection altered both the density and velocity fields in such a way that these effects were canceled in the determination of dynamic pressure.

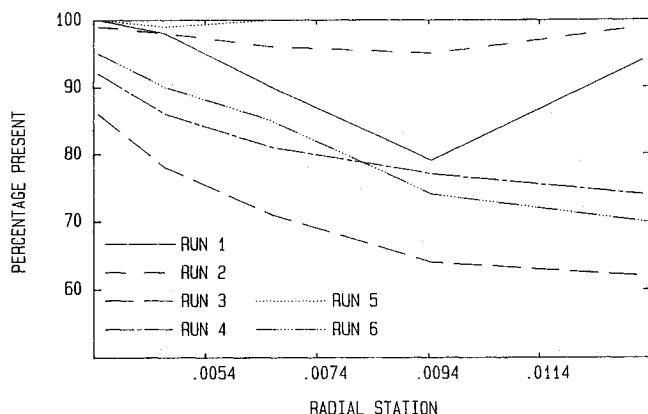


Fig. 14 Hydrogen concentration in the backflow region.

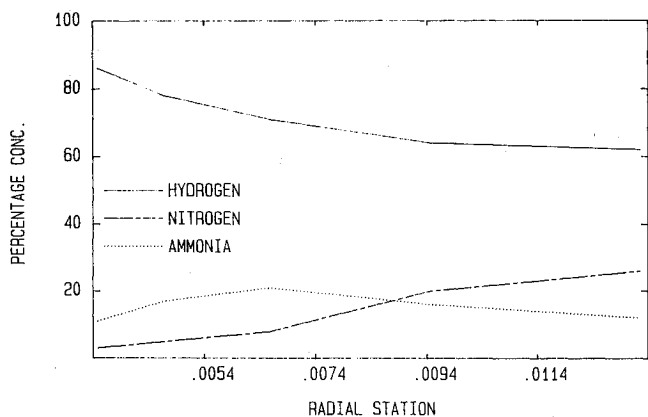


Fig. 15 Relative species abundance in the backflow region from case 3.

Inspection of Figs. 8 and 9 reveals that the assumed velocity profile has a limited effect on those properties analyzed along CD. In Fig. 10, the relative abundance of each species is plotted for the results from case 3. It is noted that as the nozzle lip is approached, moving from D toward C, the concentration of ammonia rises above that of nitrogen. Thus, it is clear that, unlike the computations performed in Ref. 4 for the isentropic core expansion of the same thruster, separation effects are found to be of great significance in the boundary-layer expansion. The trends of these calculations are in the expected direction and reflect those found by Hueser et al.<sup>5</sup>

The distribution of flow angle along CD is shown in Fig. 11. Because little difference in any of the solutions was discernible only the result from case 3 is shown. Hence, it is found that the flow angle is quite insensitive to the initial flow conditions assumed. For completeness, the degree of thermal nonequilibrium is considered by examination of Fig. 12, in which the translational, rotational, and total temperatures are plotted as a function of distance along CD. The results shown are again those obtained for case 3. By comparison with Fig. 6, it is clear that in expanding around the nozzle lip the translational and rotational modes have experienced significant departure. Indeed, the region just in front of the nozzle wall is characterized by strong rarefaction, which gives rise to the observed nonequilibrium effects. Although the contours in Fig. 12 are relatively flat, the flow should not be regarded as frozen. Significant temperature gradients exist in the direction normal to CD.

### Results in the Backflow Region

Finally, the properties along the line AB, which lies in the backflow region of the plume expansion, are considered. In Fig. 13, the dynamic pressure is shown for all six cases. It is evident that each set of initial conditions gives rise to a unique profile, especially at small distances (or large backflow angles) from the nozzle lip. It is interesting that the most realistic con-

ditions (case 3) give the largest values for the dynamic pressure. In all cases, the amount of backflow increases with an increase of the flow temperature at the nozzle wall. In Fig. 14, the relative concentrations for hydrogen are shown. These results are much more sensitive to the initial conditions than those shown in Fig. 11. Nevertheless, it is possible to group together the solutions for cases 3, 4, and 6. However, the convergence of dynamic pressure for cases 3 and 4 at large distances from the lip are not repeated in these results.

In Fig. 15, the relative abundance of each species is shown for the results obtained for case 3. Once again, as the nozzle lip is approached, the fraction of hydrogen increases and the amount of ammonia exceeds that of nitrogen. The mixture of gas found in this region of the flowfield is very different from that initially specified in Table 1. The flow angle distribution was again found to be invariant for the conditions investigated, and a sample result for case 3 is given in Fig. 16. Finally, the degree of thermal nonequilibrium present in the backflow region is evident from Fig. 17, which shows the result for case 3. It should be noted that the translational and rotational modes have undergone further separation in comparison with Fig. 12. In addition, it is evident from the flowfield calculations that the thermal modes are effectively frozen due to the very low collision rate.

### Discussion

The assumed form of the laminar boundary layer temperature profile has a direct bearing on the backflow potential of the small thruster considered. In particular, the amount of backflow is effectively specified by the gas temperature at the nozzle wall. The higher the flow temperature at the surface the greater the mass flow around the nozzle lip. These trends are also found in front of the nozzle lip. Such phenomena is to be expected as the flow in this region mainly arises as a result of

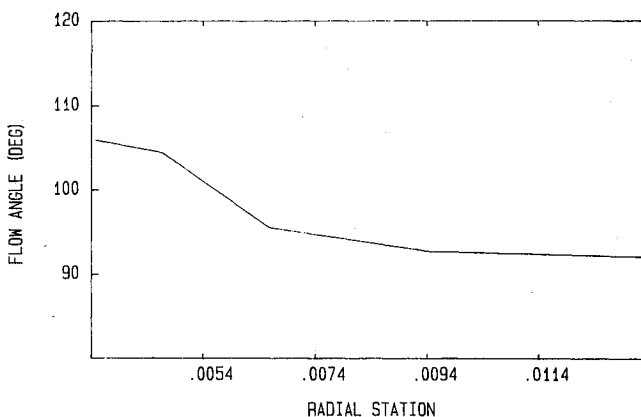


Fig. 16 Flow angle in the backflow region from case 3.

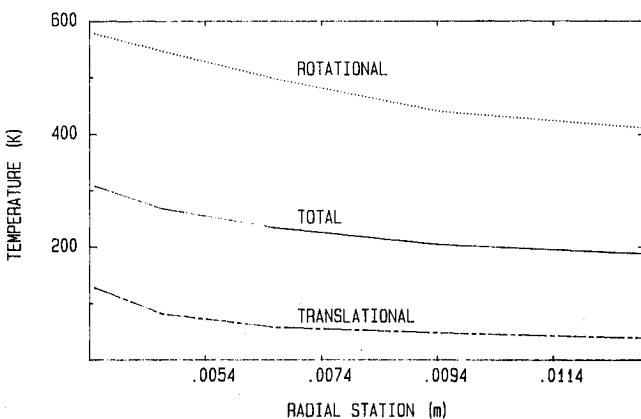


Fig. 17 Thermal nonequilibrium in the backflow region from case 3.

the thermal backscattering of molecules. This finding may have some impact on the design of nozzles in which the ability to decrease the flow temperature at the nozzle wall would certainly lead to a reduction in the impingement forces resulting from the thruster.

For a given temperature profile there are large differences observed in flowfield properties depending on whether diffuse or specular reflection is assumed along the nozzle wall. However, much smaller departures are found for variation in the wall temperature specified to the diffuse reflector model. The reliance of the amount of backflow on the wall interaction modeling in the DSMC technique highlights the requirement for improvement in this aspect of the simulation scheme. It is generally recognized that both the diffuse and specular reflectors are oversimplified models with physical reality lying somewhere between these two extremes. It is found that the influence of the conditions specified at the nozzle wall extends to 60% of the boundary layer at the nozzle exit plane.

The velocity profile assumed has a limited effect on the flow in front of the nozzle lip. Larger differences are noted for the results obtained in the backflow region. The input of different velocity profiles is found to affect directly the flow velocity in the nozzle boundary layer from the inlet plane all the way through to the nozzle exit plane.

It is generally found that the calculations in the backflow region are much more sensitive to the initially specified conditions and show significant variation when compared with those in front of the nozzle lip. This aspect of the calculations reinforces the need for parametric study such as that reported here and for the verification of such predictive methods through comparison with reliable experimental data. In the following, the measurement of various flow properties in the different regions of the expansion is discussed. Special attention is given to the determination of suitable initial starting conditions for input into the DSMC calculation.

### Experimental Considerations

Before commencing any calculations, it would be intuitively clear that the profiles initially assumed for temperature, velocity, and density would have a significant impact on the results obtained in the nozzle exit plane. What then are the prospects that these conditions can be prescribed by matching calculations such as those presented in this study against suitable experimental data? Bailey<sup>1</sup> has made pitot pressure measurements in the exit plane of a number of nozzles. Some of these have been compared with results obtained from a Navier-Stokes code,<sup>2</sup> and reasonable agreement was found. However, these investigations were made using pure gases in nozzles that have an exit radius one order of magnitude greater than that found in the thruster considered earlier.

In the region in front of the nozzle lip, it may be possible to employ nonobtrusive diagnostic techniques such as electron beam fluorescence. This method allows measurement of flow density that is proportional to the intensity of fluorescence induced in the gas. In addition, rotational temperature may be inferred from the detailed rotational-vibrational band structure. Such analysis should give useful information on the temperature profile near to the exit plane. Unfortunately, the results computed for the different surface models are too similar in this region of the flow to allow any firm conclusions to be drawn. In the consideration of making use of the rotational temperatures calculated with the DSMC method, it should be noted that, although the general appearance of these profiles is correct, they may be inaccurate in detail. The use of the standard Larsen-Borgnakke energy exchange model<sup>9</sup> assumes that the probability of rotational energy transfer is independent of both species and local flow conditions. This represents a limitation on the model with which an unknown error must be associated. This aspect of DSMC calculations has recently been improved by Boyd<sup>14</sup> with the introduction of an ex-

change probability, which is defined in terms of the collision energy.

The results obtained in the backflow region for dynamic pressure seem to offer the best opportunity for determination of the correct form for the initial flow conditions. In Fig. 13, each case investigated gave rise to a unique solution. The differences are particularly noticeable at small distances from the nozzle lip. The measurement of the degree of species separation would also be desirable. Unfortunately, experimental investigation of the backflow region presents technical difficulties. First, the flow properties will clearly be very sensitive here to the background pressure obtained in the vacuum facility. Second, in the flow angle measurements of Bailey,<sup>1</sup> an effect is sometimes found whereby the scattering of molecules from the measuring device becomes significant. However, provided that both of these possible sources of error are overcome, it should be possible to determine accurately the required quantities from probe and quartz crystal microbalance (QCM) measurements. The free molecular probe employed by Bailey has good accuracy down to  $1.3 \times 10^{-3}$  Pa, which is well within the range of pressures encountered in Fig. 13. QCMs are used to measure the mass flux of the different species, although the detection of hydrogen is usually impossible. It is therefore proposed that it is possible to determine the most appropriate nature of the initial flow conditions by comparison with direct measurement of pressure and species concentrations in the backflow region.

### Conclusions

In the computation of the nozzle lip and backflow regions of a small hydrazine thruster plume, it has been shown that significant species separation and thermal nonequilibrium effects occur as the gas expands into the vacuum of space. Such phenomena cannot normally be simulated with traditional continuum methods. It is therefore concluded that application of the more numerically intensive DSMC technique is required for the accurate prediction of such flowfields. The sensitivity of the computed results to assumptions made regarding the initial state of the gas has been assessed and found to be particularly important in the backflow region. This aspect of the calculations provides the best opportunity for experimental verification of the type of results obtained in the present study. It is found that the impingement potential of the thruster in the backflow region is determined largely by the flow temperature at the nozzle wall. Suitable design alterations to the nozzle that could effect a reduction in this temperature would therefore lead to a corresponding decrease in the impingement effects associated with the thruster.

### References

- 1 Bailey, A. B., "Flow Angle Measurements in a Rarefied Nozzle Plume," *AIAA Journal*, Vol. 25, No. 10, 1987, pp. 1301-1304.
- 2 Cooper, G. K., Jordan, J. L., and Phares, W. J., "Analysis Tool for Application to Ground Testing of Highly Underexpanded Nozzles," *AIAA Paper 87-2015*, June 1987.
- 3 Doo, Y. C., and Nelson, D. A., "Analysis of Small Bipropellant Engine Internal Flows by the Direct Simulation Monte Carlo Method," *AIAA Paper 87-1548*, June 1987.
- 4 Boyd, I. D., and Stark, J. P. W., "Assessment of Impingement Effects in the Isentropic Core of a Small Satellite Control Thruster Plume," *Proceedings of the Institution of Mechanical Engineers, Part G: Journal of Aerospace Engineering*, Vol. 203, 1989, pp. 97-103.
- 5 Hueser, J. E., Melfi, L. T., Bird, G. A., and Brock, F. J., "Rocket Nozzle Lip Flow by Direct Simulation Monte Carlo Method," *Journal of Spacecraft and Rockets*, Vol. 23, No. 4, 1986, pp. 363-367.
- 6 Campbell, D. H., "Nozzle Lip Effects on Argon Expansions into the Plume Backflow," *Journal of Spacecraft and Rockets*, Vol. 26, No. 4, 1989, pp. 285-292.
- 7 Bird, G. A., *Molecular Gas Dynamics*, Clarendon, Oxford, 1976.

<sup>8</sup>Bird, G. A., "Direct Simulation of Gas Flows at the Molecular Level," *Communications in Applied Numerical Methods*, Vol. 4, 1988, pp. 165-172.

<sup>9</sup>Borgnakke, C., and Larsen, P. S., "Statistical Collision Model for Monte Carlo Simulation of Polyatomic Gas Mixtures," *Journal of Computational Physics*, Vol. 18, 1975, pp. 405-420.

<sup>10</sup>Boyd, I. D., and Stark, J. P. W., "A Comparison of the Implementation and Performance of the Nanbu and Bird Direct Simulation Monte Carlo Methods," *Physics of Fluids*, Vol. 30, No. 12, 1987, pp. 3661-3668.

<sup>11</sup>Boyd, I. D., "Monte Carlo Simulation of an Expanding Gas," *Computers in Physics*, Vol. 3, No. 3, 1989, pp. 73-76.

<sup>12</sup>Bird, G. A., "Thermal and Pressure Effects in High Altitude Flows," AIAA Paper 88-2732, June 1988.

<sup>13</sup>Moss, J. N., Cuda, V., and Simmonds, A. L., "Nonequilibrium Effects for Hypersonic Transitional Flows," AIAA Paper 87-0404, Jan. 1987.

<sup>14</sup>Boyd, I. D., "Rotational-Translation Energy Transfer in Rarefied Nonequilibrium Flows," *Physics of Fluids A*, Vol. 2, No. 3, 1990, pp. 447-452.

### Recommended Reading from the AIAA

*Progress in Astronautics and Aeronautics Series . . .* 

## Dynamics of Explosions and Dynamics of Reactive Systems, I and II

J. R. Bowen, J. C. Leyer, and R. I. Soloukhin, editors

Companion volumes, *Dynamics of Explosions* and *Dynamics of Reactive Systems, I and II*, cover new findings in the gasdynamics of flows associated with exothermic processing—the essential feature of detonation waves—and other, associated phenomena.

*Dynamics of Explosions* (volume 106) primarily concerns the interrelationship between the rate processes of energy deposition in a compressible medium and the concurrent nonsteady flow as it typically occurs in explosion phenomena. *Dynamics of Reactive Systems* (Volume 105, parts I and II) spans a broader area, encompassing the processes coupling the dynamics of fluid flow and molecular transformations in reactive media, occurring in any combustion system. The two volumes, in addition to embracing the usual topics of explosions, detonations, shock phenomena, and reactive flow, treat gasdynamic aspects of nonsteady flow in combustion, and the effects of turbulence and diagnostic techniques used to study combustion phenomena.

**Dynamics of Explosions**  
1986 664 pp. illus., Hardback  
ISBN 0-930403-15-0  
AIAA Members \$54.95  
Nonmembers \$92.95  
Order Number V-106

**Dynamics of Reactive Systems I and II**  
1986 900 pp. (2 vols.), illus. Hardback  
ISBN 0-930403-14-2  
AIAA Members \$86.95  
Nonmembers \$135.00  
Order Number V-105

**TO ORDER:** Write, Phone or FAX: American Institute of Aeronautics and Astronautics, c/o TASC0,  
9 Jay Gould Ct., P.O. Box 753, Waldorf, MD 20604 Phone (301) 645-5643, Dept. 415 FAX (301) 643-0159

Sales Tax: CA residents, 7%; DC, 6%. Add \$4.75 for shipping and handling of 1 to 4 books (Call for rates on higher quantities). Orders under \$50.00 must be prepaid. Foreign orders must be prepaid. Please allow 4 weeks for delivery. Prices are subject to change without notice. Returns will be accepted within 15 days.